ACS OMEGA

http://pubs.acs.org/journal/acsodf
Article

Urinary IR700 Ligand as an Early Biomarker of Therapeutic Efficacy of Near-Infrared Photoimmunotherapy

Shuhei Okuyama, Daiki Fujimura, Aki Furusawa, Hiroshi Fukushima, Ryuhei Okada, Tairo Ogura, Masayuki Nishimura, Peter L. Choyke, and Hisataka Kobayashi*

Cite This: *ACS Omega* 2025, 10, 6983−6991
Read Online

ABSTRACT: Near-infrared photoimmunotherapy (NIR-PIT) is a cell-selective cancer therapy employing monoclonal antibody-photoabsorber conjugates (APCs) and near-infrared (NIR) light. When exposed to NIR light, the photoabsorber, IR700, releases an axial ligand, resulting in a transition of the remaining molecule from water-soluble to hydrophobic. This results in the death of APC-bound cells by physical damage to the cell membrane. The amount of released IR700 ligand reflects the completeness of the photochemical reaction and, therefore, can be a biomarker for treatment efficacy. In this study, we developed and validated a quantitative analytic method for detecting excreted IR700 ligands in urine using a liquid chromatograph-triple quadrupole mass spectrometer (LC-MS/MS). In A431 tumor-bearing mice treated with NIR-PIT, the urinary ligand increased with increasing the light dose, which was positively correlated with the loss of fluorescence and therapeutic effects. This study suggests that quantitative analysis of urinary ligands using LC-MS/MS can be a rapid biomarker of NIR-PIT efficacy.

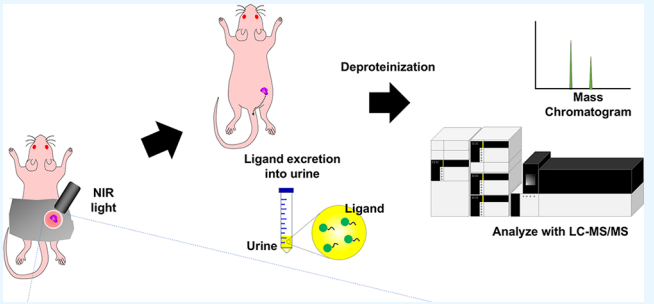

Near-infrared photoimmunotherapy (NIR-PIT) is a new cancer treatment that uses a combination of tumor-targeting antibodies conjugated with a near-infrared (NIR)-light-sensitive dye (IRDye700DX, abbreviated as IR700) and NIR laser irradiation.[1] The antibody-photoabsorber conjugates (APCs) are bound to antigens on the surface of tumor cells and are activated by 690 nm light illumination. The APCs are initially hydrophilic; however, they immediately become hydrophobic after the photochemical release of hydrophilic axial ligands.[2] This reaction causes aggregation of antibody−antigen complexes that induce physical stress to the cellular membrane, impairing membrane function. Membrane damage leads to cell swelling and eventually bursting, resulting in the induction of rapid immunogenic cell death (ICD).[3] Since ICD occurs only on cells to which a sufficient number of APCs have bound and have then been exposed to NIR light, this therapy selectively eliminates cancer cells without affecting the surrounding target-negative cells. NIR-PIT has demonstrated its efficacy in human patients with unresectable locally advanced or recurrent head and neck cancer using Akalux (Rakuten Medical Inc., San Diego, CA, USA), an epidermal growth factor receptor (EGFR)-targeted APC, and a 690 nm laser system (BioBlade, Rakuten Medical Inc.) with clinical approval in Japan in 2020.[4] In addition, a global phase III clinical trial of NIR-PIT with ASP-1929, a conjugate of cetuximab and IR700, is ongoing in patients with recurrent head and neck squamous cell carcinoma.[5]

Conventional cancer treatments, such as radiation therapy and chemotherapy, are dose-limited because they cause damage to normal cells. On the other hand, NIR-PIT can be performed repeatedly without limitation due to its high selectivity. NIR-PIT has high cell selectivity because only cells with the appropriate antigen are killed. The administered APCs remain in the circulation after NIR-PIT and reaccumulate in the tumor 3 to 24 h after light exposure, allowing retreatment without additional drug administration.[6,7] However, it may be difficult to visually assess efficacy in real time. To date, no promising biomarker for estimating the early therapeutic effect has been developed.

In the clinical setting, the treatment efficacy of solid tumors is generally evaluated based on response evaluation criteria in solid tumors (RECIST).[8,9] In this method, tumors are imaged by computed tomography (CT) or magnetic resonance imaging (MRI) before and several weeks after treatment to determine the tumor response. In an NIR-PIT clinical trial, tumor responses were determined by imaging after 4 weeks of treatment based on a modified RECIST 1.1.[10,11]

Currently available methods of early assessment after NIR-PIT include positron emission tomography (PET) using

Received: October 29, 2024
Revised: January 8, 2025
Accepted: January 14, 2025
Published: February 13, 2025

https://doi.org/10.1021/acsomega.4c09850
ACS Omega 2025, 10, 6983−6991

fluorine-18-fluorodeoxyglucose (^{18}F-FDG) but these are expensive and cumbersome.[12] In addition, studies are underway to evaluate early efficacy by monitoring the fluorescence intensity on the tumor using the attenuation of fluorescence intensity on the tumor as a function of light irradiation in NIR-PIT.[13−15] Further diagnostics include analyzing biomarker proteins such as heat shock protein (HSP)/70, HSP/90, and calreticulin, which are released into the tumor microenvironment after NIR-PIT-induced ICD.[16−18] However, quantification methods for these biomarkers are not yet established.

We hypothesized that hydrophilic axial ligands released from the IR700 molecule after exposure to NIR light could act as biomarkers of treatment efficacy. Therefore, the purpose of this study is to evaluate the feasibility of using the detection of urinary hydrophilic ligands released from APCs as an indicator of early therapeutic efficacy after NIR-PIT. In this study, we show that it is possible to detect ligands in mouse urine using a liquid chromatography-triple quadrupole mass spectrometer (LC-MS/MS). Also, quantitative analysis of excreted ligands before and after NIR-PIT treatment was performed using the human EGFR-expressing A431 tumor mouse model, and correlation with fluorescence intensity on the tumor, which attenuates as the treatment progresses, was analyzed using a fluorescence monitoring system.

RESULTS AND DISCUSSION

To ensure the validity of the results obtained by LC-MS/MS, we based our validation on the following criteria: (1) selectivity; (2) carryover; (3) linearity and calibration standard; (4) precision and accuracy in inter- and intra-assays; (5) recovery rate; and (6) stability.[19]

The selectivity test was performed by analyzing samples containing either the ligand or the internal standard (IS) using LC-MS/MS to ensure that there were no interfering peaks. The ligand showed a retention time of 3.8 min with no interfering peaks using multiple reaction monitoring (MRM) chromatograms (Figure 1A,B). Also, no interfering peak for IS at the retention time of 3.8 min was observed (Figure 1C,D). These results showed that ligand and IS can be analyzed under this method without interference from other peaks.

The carryover test was performed by analyzing three replicates for the axial ligand immediately after a high concentration (200 μg/L) analysis. The carryover was calculated as the percent response in the blank urine relative to that in the preceding sample. In this analysis, no carryover was observed, confirming negligible levels of carryover that influenced this analysis.

Regarding the linearity and calibration standard, to confirm that the ligands detected by LC-MS/MS were within the linearity range of the calibration curve, calibration standard samples with a ligand concentration at 0 μg/L, the lower limit of quantitation (LLOQ; 5 μg/L) and others (10, 20, 50, 100, and 200 μg/L) were analyzed by LC-MS/MS to generate a calibration curve based on the linear regression model using LabSolusions software (Shimadzu Corp., Kyoto, Japan). The calibration plot of weighting was done by using the 1/concentration method. The calibration fit formulas of the triplicate runs were as follows; Day 1, $Y = 0.0627X + 0.0211$ ($r = 0.997$); Day 2, $Y = 0.0585X + 0.00507$ ($r = 0.997$); and Day 3, $Y = 0.0750X + 0.0434202$ ($r = 0.996$) (r: correlation coefficient). The accuracy at LLOQ was 90.0−116.0%, and at other concentrations (10.0−200.0 μg/L), they were 85.4−115.0% at

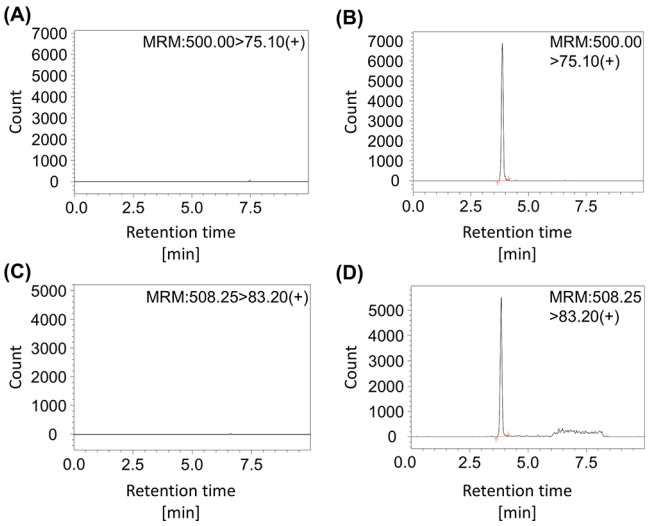

Figure 1. Multiple reaction monitoring (MRM) chromatogram of the ligand and IS in a selectivity test obtained from LC-MS/MS. The ligand peak (fragment m/z 75.10 from parent 500.00, retention time 3.86 min) was observed at the LQC (2.5 μg/L) sample. The horizontal axis shows the retention time (min), and the vertical axis shows the ion count. The red lines show the baseline of the assigned peak. Representative chromatograms from the (A) control blank sample, (B) ligand-added mouse urine, (C) blank sample of IS, and (D) IS (fragment m/z 83.20 from parent 508.25, retention time 3.83 min).

day 1 through day 3 (Table S2), indicating well-fitted calibration curves with high reproducibility even at the LLOQ.

The intraday and interday precision and accuracy of ligand detection by LC-MS/MS were determined by analyzing five sets of mouse urine samples at the LLOQ (5.0 μg/L), low quality control (LQC) (15.0 μg/L), medium quality control (MQC) (75.0 μg/L), and high quality control (HQC) (150.0 μg/L) of axial ligand concentrations on three different days. Precision and accuracy data were obtained as follows: Day 1, 7.0 and 104.8% at the LLOQ, 3.2−5.6 and 97.3−102.9% at other concentrations; Day 2, 10.1 and 115.5% at the LLOQ, 5.0−12.0 and 101.1−108.5% at other concentrations; Day 3, 12.9 and 109.7% at the LLOQ, 1.1−5.9 and 102.3−109.8% at other concentrations; intra-assay ($N = 15$), 10.4 and 110.0% at the LLOQ, 5.1−7.3 and 100.9−107.0% at other concentrations (Table S3). According to the bioanalytical method validation,[19] the criteria of precision are ±20% at the LLOQ and ±15% at other concentrations at 3-day interday analysis; the most accurate were 80−120% at the LLOQ and 85−115% at other concentrations at 3-day interday analysis. Since the results achieved these criteria, it confirmed that the analysis could be performed with sufficient precision and accuracy in these concentration ranges.

The ligand recovery rate was evaluated based on quantitative values obtained from the LC-MS/MS analysis results of mouse urine spiked with the 50 μg/L axial ligand and treated for deproteinization. The recovery rate was 103.2% ± 4.4 ($n = 5$; mean ± standard error of the mean (SEM)). This result suggests that the pretreatment for this ligand analysis does not result in the loss of the axial ligand analyte.

The stability of the samples at the LQC and HQC concentrations was tested using samples at each group in the following conditions: (1) five freeze−thaw cycles at −80 °C with at least 12 h of frozen time; (2) short-term storage at room temperature for 24 h; (3) long-term storage at −80 °C for 15 days; (4) samples pretreated for LC-MS/MS analysis at 4 °C for

https://doi.org/10.1021/acsomega.4c09850
ACS Omega 2025, 10, 6983−6991

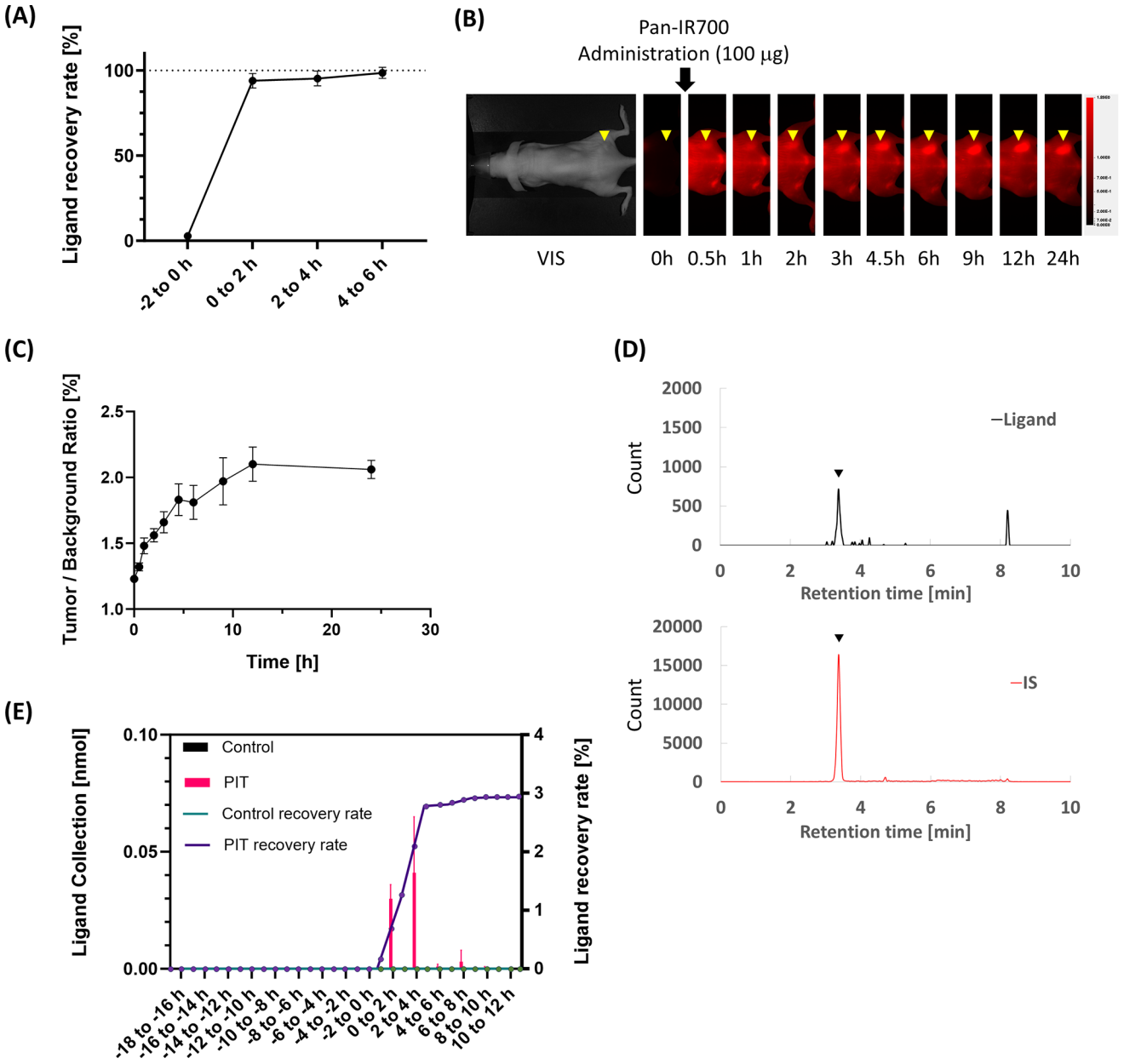

Figure 2. Confirmation of the timing of the release of the ligand into mouse urine by LC-MS/MS. (A) LC-MS/MS analysis of ligand levels in urine collected before and after intravenous injection of the ligand ($n = 4$; mean ± SEM). (B) Biodistribution of Pan-IR700. (C) Tumor-background ratio of fluorescence intensity after 100 μg of Pan-IR700 administration ($n = 3$; mean ± SEM). (D) Representative examples of the MS chromatogram of the ligand and IS from NIR-PIT-treated mice urine. (E) Ligand detection and recovery rate vs dose by LC-MS/MS from mouse urine before and after NIR-PIT with Pan-IR700 ($n = 3$; mean ± SEM for ligand detection; mean for recovery rate).

24 h; and (5) 48 h. The accuracy of LQC and HQC in each test is shown in Table S4. The minimal acceptance criterion for this study was an accuracy of ±15% of nominal concentration under all conditions, suggesting that the ligand is stable in all storage environments. In this study, samples were subjected to LC-MS/MS analysis immediately after pretreatment.

To determine when the ligand is excreted into the urine, we directly injected the axial ligand standards intravenously into mice and collected mouse urine over time. As shown in Scheme S1A, we collected mouse urine before and after ligand administration at 2 h intervals and quantitatively evaluated the ligand in the urine. The ligand in each urine sample was quantitatively analyzed by LC-MS/MS, and the recovery rate was determined by calculating the ratio of the measured amount to the amount of ligand administered. The integrated ligand recovery at each time point was as follows: 2.784 ± 1.013% at −2 to 0 h, 93.918 ± 4.244% at 0 to 2 h, 95.240 ± 4.361% at 2 to 4 h, and 98.560 ± 3.209% at 4 to 6 h ($n = 4$; mean ± SEM), suggesting that almost all of the ligand in the bloodstream was rapidly excreted in the urine by 2 h after administration (Figure 2A).

Next, we examined the biodistribution of panitumumab-IR700 (Pan-IR700) in tumors to determine the time of maximum APC accumulation. The biodistribution was examined by imaging the drug distribution in the tumor up to 24 h after Pan-IR700 administration to mice. The tumor-to-background ratio (TBR) was calculated by placing a region of interest in the tumor and contralateral site, respectively. The TBR values

https://doi.org/10.1021/acsomega.4c09850
ACS Omega 2025, 10, 6983−6991

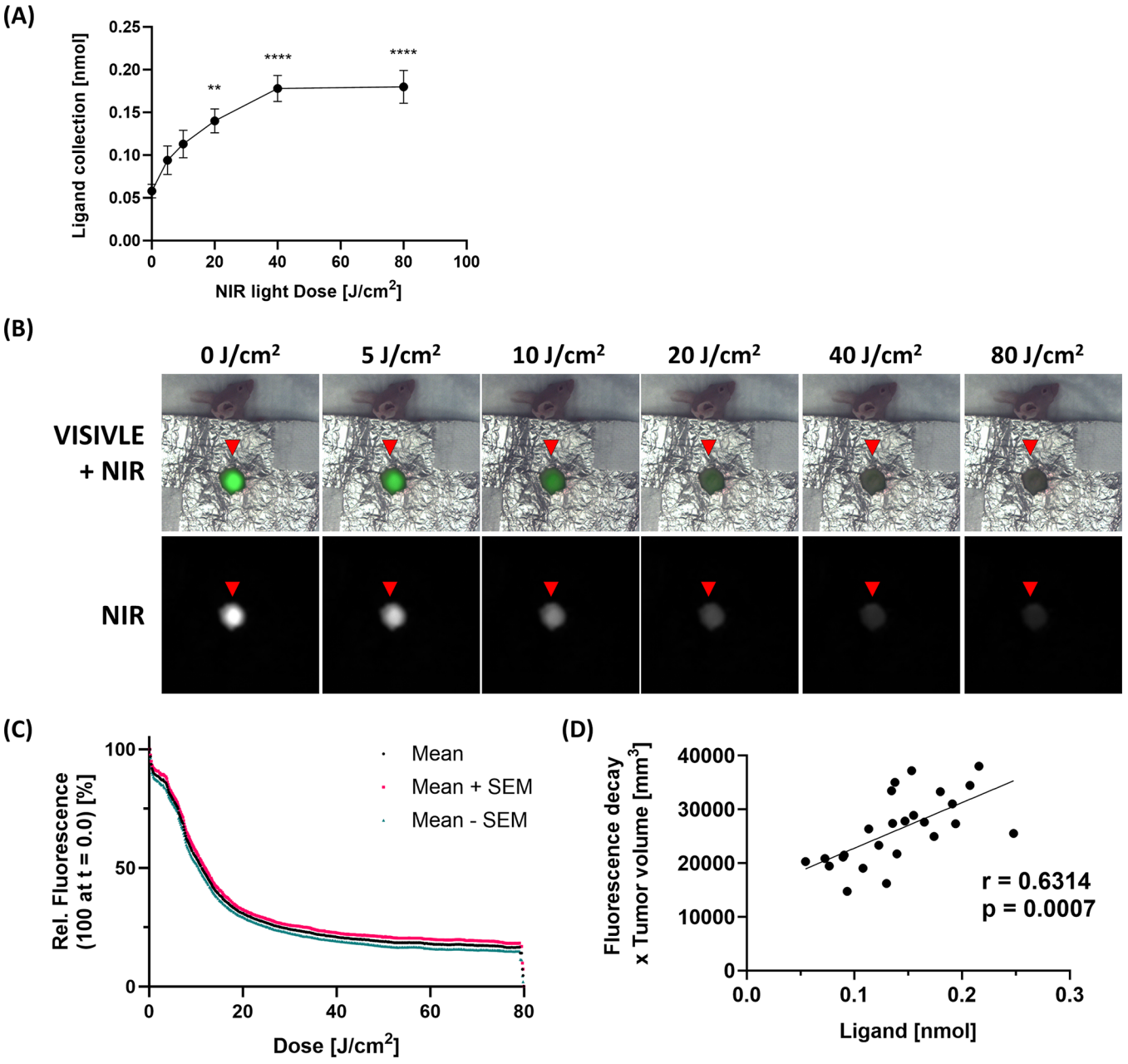

Figure 3. Changes in the urinary ligand and fluorescence intensity during NIR-PIT performed on A431 tumors in mice. (A) Ligand amounts detected by LC-MS/MS from mouse urine subjected to NIR-PIT at various NIR light doses (n = 5 per group; mean ± SEM; **, $p < 0.01$; ****, $p < 0.0001$; vs 0 J/cm^2; one-way analysis of variance (ANOVA) followed by the Dunnett's test). (B) Representative examples of visible and fluorescence images at 0, 5, 10, 20, 40, and 80 J/cm^2 light exposure. (C) Decay curves of relative fluorescence intensity upon light irradiation (n = 7; mean and mean ± SEM). (D) Correlation between the amount of ligand detected by LC-MS/MS in mouse urine after NIR-PIT and the fluorescence decay ratio during NIR-PIT (n = 25; r = 0.6314; p = 0.0007; Pearson's product moment correlation coefficient).

from this study were 1.23 ± 0.02, 1.32 ± 0.03, 1.48 ± 0.06, 1.56 ± 0.05, 1.66 ± 0.08, 1.83 ± 0.12, 1.81 ± 0.13, 1.97 ± 0.18, 2.10 ± 0.13, and 2.06 ± 0.07% at 0, 0.5, 1, 2, 3, 4.5, 6, 9, 12, and 24 h after administration of Pan-IR700, respectively (n = 3; mean ± SEM). TBR reached its maximum at about 12 h after APC administration and was maintained thereafter (Figure 2B,C). Therefore, in the experiments described below, NIR-PIT was performed 12−24 h after APC administration.

After administration of APC, we evaluated the timing of ligand excretion into mouse urine before and after NIR-PIT as shown in the experimental schema of Scheme S1B. A representative chromatogram showing the ligand and added IS in a mouse urine sample is shown in Figure 2D. No ligand was detected in the samples from the control and pre-PIT treatment groups, while small amounts of ligand corresponding to about 3% of the administered APCs were detected in urine from the PIT-treated group up to 8 h after NIR-PIT (Figure 2E). The results confirm that the ligand release from Pan-IR700 triggered by NIR-PIT is excreted in the urine within a few hours after irradiation.

Next, to determine the relationship between the amount of ligand detected in mouse urine and the amount of therapeutic light dose, NIR-PIT was performed at different light doses, and the urinary ligand was quantitatively analyzed by LC-MS/MS. The scheme of this study is shown in Scheme S1C. As shown in

https://doi.org/10.1021/acsomega.4c09850
ACS Omega 2025, 10, 6983−6991

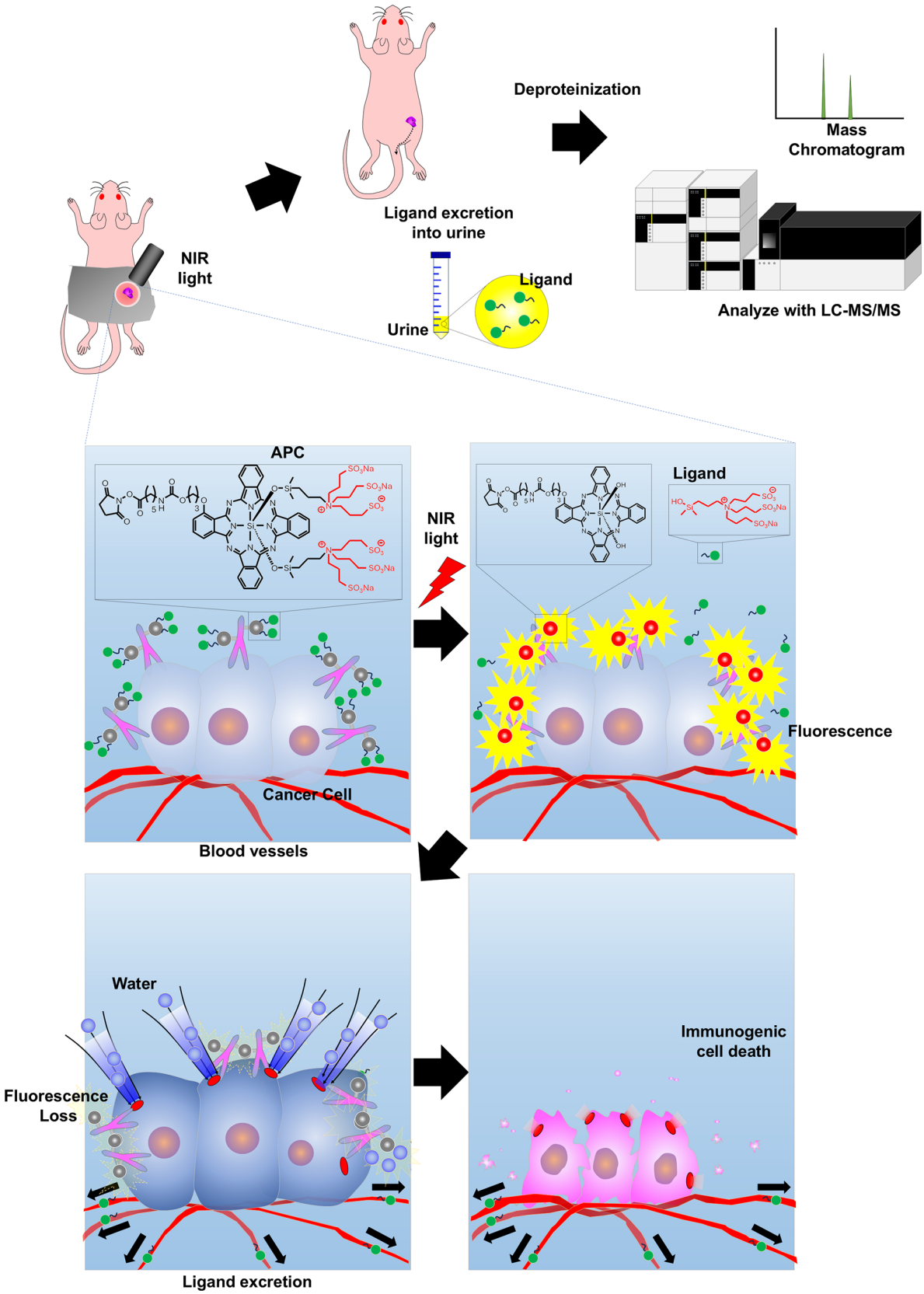

Figure 4. Schema of photoinduced ligand detection in urine using LC-MS/MS after NIR-PIT. The released ligand is excreted into urine through blood vessels and can be quantitatively detected by LC-MS/MS.

Figure 3A, the amount of ligand at each light dose increased in a light intensity-dependent manner immediately after light irradiation: 0.058 ± 0.018 nmol at 0 J/cm^2, 0.094 ± 0.037 nmol at 5 J/cm^2, 0.113 ± 0.036 nmol at 10 J/cm^2, 0.140 ± 0.031 nmol at 20 J/cm^2, 0.178 ± 0.034 nmol at 40 J/cm^2, and 0.180 ± 0.043 nmol at 80 J/cm^2 (n = 4; mean ± SEM). The amount of

https://doi.org/10.1021/acsomega.4c09850
ACS Omega 2025, 10, 6983−6991

ligand significantly increased at 20 J/cm^2 irradiation compared to the 0 J/cm^2 sample and remained constant after 40 J/cm^2, suggesting that the photochemical reaction that releases the ligand is completed at about 40 J/cm^2 under these experimental conditions.

The fluorescence generated from the APCs bound to the tumor during irradiation with therapeutic light was also observed simultaneously (Figure 3B). The fluorescence intensity on the tumor decreased in a light intensity-dependent manner, reaching a plateau at approximately 30−40 J/cm^2 (Figure 3C). A positive correlation (r = 0.6314, p = 0.0007) was observed between the amount of urinary ligand detected and the rate of loss of fluorescence intensity (Figure 3D). These results suggest that the amount of ligand in mouse urine after treatment may reflect the treatment effect of NIR-PIT confirming fluorescence intensity monitoring during treatment.

The localized and specific cytotoxicity induced by NIR-PIT is caused by a photochemical reaction in which APCs bound to antigens on the cell membrane after exposure to NIR light release axial ligands, thus, changing the property of the remaining IR700 molecule from hydrophilic to hydrophobic.[3] It has been reported that the released ligand is excreted in the urine after NIR irradiation. In this study, we established and validated a quantitative analysis method using LC-MS/MS for urinary ligands generated by NIR-PIT to evaluate the progress of cell killing by NIR-PIT for early therapeutic evaluation (Figure 4).

NIR-PIT was performed after Pan-IR700 had accumulated on mouse A431 tumors, and results showed that the ligand was excreted in the urine within 4 h after light exposure (Figure 2E). The ligand recovery was about 3% of the expected ligand amount based on the injected APC, while the reported accumulation rate of panitumumab for A431 at 24 h after administration was about 15−20% of the injected dose (ID)/g.[20,21] Although the amount of urinary ligand is small, it is sufficient for detection by LC-MS/MS. As the tumors used in this experiment were 300−600 mm^3 and weighed approximately 250 mg on average, 4−5% ID of panitumumab accumulated in the tumors is assumed. The ligand recovered from mouse urine after NIR-PIT was significantly increased compared to pretreatment, suggesting that it may well be used to estimate treatment efficacy.

The amount of ligand in mouse urine after NIR-PIT increased linearly with light irradiation, then slowed down, and reached a plateau at 40 J/cm^2 (Figure 3A). Based on the mechanism of NIR-PIT,[3] phthalocyanine groups from which the ligand dissociates by light irradiation polymerize with neighboring phthalocyanine groups. The ability to emit fluorescence is lost in the process of damaging the cell membrane. Therefore, from the results of this experiment, it can be interpreted that unreacted APCs gradually decreased, and at about 40 J/cm^2, the photochemical reaction of APCs in the tumor and surrounding tissue was completed with no further expectation of ligand release. During NIR-PIT treatment of mice with A431 tumors, fluorescence intensity rapidly decreased after starting the NIR light and then slowed down at light doses of 20−40 J/cm^2, before reaching a plateau (Figure 3B,C).

This result is consistent with the pattern of urinary ligand detection with respect to the light dose, and a positive correlation was observed between the amount of ligand detected and the rate of decay of fluorescence intensity (Figure 3D). Since the loss of fluorescence on the tumor and the release of ligand from the APC are triggered by the same photochemical reaction and, additionally, we previously published that the loss of fluorescence on the tumor positively related to therapeutic outcome of NIR-PIT,[3] it is expected from the present results that both methods will be complementary analytical methods to confirm the completeness of the photochemical reaction. Both techniques are important because it is not always feasible to monitor fluorescence.

Measuring the completeness of NIR-PIT by detecting urinary ligands and monitoring fluorescence intensity is important because conventional RECIST criteria, which are based on the size of the tumor after several weeks of treatment, are slow and may be unreliable due to posttreatment edema.[22] In contrast, released ligand amount can be analyzed using urine within hours of treatment, and fluorescence intensity monitoring can provide results during the treatment. These rapid treatment assessments provide feedback to the surgeon regarding subsequent light exposure to treat residual disease. Multiple light exposures take advantage of the Super Permeability and Retention (SUPR) effect after a single NIR-PIT treatment.[6,23] A clinical trial is currently underway to determine the feasibility of monitoring fluorescence intensity during NIR-PIT in human patients.[24]

There are several limitations to this study. First, a low amount of ligand was detected in the absence of light irradiation, as shown in Figure 3A. Since blood ligands are rapidly excreted in urine, it is possible that the ligand in the mouse urine at 0 J/cm^2 was released from the APC by metabolism just before the urine sample was collected. To confirm that the detected ligand is due to NIR-PIT, the ligand in the urine before light irradiation should be measured as a baseline. Second, the results of this study were obtained by treating mice with subcutaneously implanted tumors, which consistently grew and were technically easy to be treated. In clinical practice, human tumors are larger than those of mice and may excrete markedly different ligand levels. Future studies using urine samples from humans who have undergone NIR-PIT are needed to determine appropriate thresholds.

In summary, this study performed a quantitative analysis of urinary ligands excreted into urine after NIR-PIT. Ligands in mouse urine increased in a light dose-dependent manner, reaching a plateau at a certain light dose, and confirmed the results of a concurrent fluorescence intensity monitoring study, suggesting that urinary ligand reflects the degree of photochemical reaction during NIR-PIT. Future studies using urine samples from human patients treated with NIR-PIT are warranted to determine its clinical applicability.

MATERIALS AND METHODS

Chemicals and Reagents. The water-soluble silica-phthalocyanine dye IR700 ($C_{74}H_{96}N_{12}Na_4O_{27}S_6Si_3$, molecular weight 1954.22) was purchased from LI-COR Bioscience (Lincoln, NE). A fully humanized IgG2 monoclonal antibody against human EGFR, panitumumab, was purchased from Amgen (Thousand Oaks, CA, USA). An axial ligand standard ($C_{14}H_{34}ClNO_{10}S_3Si$, molecular weight of 536.14) and internal standard ($C_{12}{}^{13}C_2H_{28}D_6ClNO_{10}S_3Si$, molecular weight of 544.13, abbreviated as IS) were obtained from Alsachim (Illkirch-Graffenstaden, France). All other chemicals were reagent-grade.

Preparation of Samples for LC-MS/MS Analysis. Stock solutions of the axial ligand and IS were separately prepared in methanol at a concentration of 10,000 mg/L and 12,000 mg/L, respectively, from powder. Two working solutions containing the axial ligand or IS at concentrations of 100 mg/L were

https://doi.org/10.1021/acsomega.4c09850
ACS Omega 2025, 10, 6983−6991

prepared in 1% (v/v) formic acid in methanol by mixing and diluting first stock solutions at 10,000 mg/L and 12,000 mg/L, respectively. Aliquots of first stock solutions were stored at −80 °C.

Urine collected from some healthy nude mice was diluted 6-fold with methanol containing 1% formic acid and centrifuged at 14,000 rpm to collect the supernatant. This supernatant was used as a diluent for the standard solution preparation. Calibration standard samples were prepared by adding different volumes of the second stock solutions of the axial ligand to reach final concentrations of 5, 10, 20, 50, 100, and 200 μg/L. IS solution was added to each solution to reach a final concentration of 100 μg/L. Quality control samples for validation in urine (200 μL) were prepared by adding different volumes of the second stock solutions of the axial ligand and IS to reach final concentration levels at LQC, 15 μg/L; MQC, 75 μg/L; and HQC, 150 μg/L.

LC-MS/MS Analysis. A Nexera X2 UHPLC system coupled to a triple quadrupole mass spectrometer (LCMS-8060, Shimadzu Corp.) was used for quantitative analysis of the axial ligand in the urine sample. In brief, the mobile phase consisting of 20 mmol/L ammonium formate in water (A) and acetonitrile (B) was delivered at a flow rate of 0.4 mL/min. The gradient conditions were set as 1% B (0.0 min), 40% B (5.0 min), 98% B (5.1−7.0 min), 1% B (7.1−10.0 min), and STOP (10.0 min). The injection volume was 2 μL. Chromatographic separation was achieved on a Scherzo SM-C18 column (2.0 mm i.d. × 150 mm L, 3 μm, Imtakt, Portland, OR, USA). The column oven temperature was set at 40 °C. The LCMS-8060 parameters were set as follows: ESI positive mode, probe voltage of +4.0 kV, nebulizing gas flow rate of 2.0 L/min, drying gas flow of 10 L/min, heating gas flow of 10 L/min, DL temperature of 250 °C, and block heater temperature of 400 °C. MRM transitions adapted in this study and examples of the LC-MS/MS spectra of the ligand and IS in mouse urine are shown in Table S1 and Figure S1, respectively.

Synthesis of Panitumumab-IR700 Conjugation. Panitumumab was conjugated with IR700 according to a previously published protocol.[25] We abbreviated panitumumab-IR700 as Pan-IR700.

Cell Culture. A431 luciferase cells expressing human EGFR were cultured as shown in the previous paper.[1]

Animal and Tumor Models. All animal experiments were approved by the Animal Care and Use Committee of the National Cancer Institute. Six- to eight-week-old female homozygote athymic nude mice (strain #553) were purchased from Charles River (NCI-Frederick, Frederick, MD, USA). During the procedure, mice were anesthetized with inhaled 2−3% isoflurane. To determine the tumor volume, the greatest longitudinal diameter (length) and the greatest transverse diameter (width) were measured with an external caliper. Tumor volumes were calculated using the following formula: tumor volume (mm^3) = length (mm) × $width^2$ (mm^2) × 0.5.

Evaluation of Ligand Excretion Time into Urine. A431 cells (2×10^6) were injected subcutaneously in the right dorsal cortex of the mice. Tumors were studied after they reached volumes of 300 to 600 mm^3. To determine the extent to which the ligand entering the bloodstream is eliminated from the body and the timing of this elimination, 1.2 ng of ligand was intravenously administered into A431 tumor-bearing mice (n = 4). Urine samples were collected every 2 h starting 2 h before the treatment to 6 h after administration (Scheme S1A).

To detect the ligand released from IR700 and excreted into the urine, mice having A431 tumors at 50 to 100 mm^3 were divided into two groups with three animals each. Pan-IR700 (100 μg) was intravenously administered only to the NIR-PIT group, and 16 h later, NIR light of 80 J/cm^2 was irradiated only to the tumor of the NIR-PIT group; urine was collected every 2 h from 18 h before to 12 h after NIR-PIT (Scheme S1B).

To investigate the therapeutic effect of in vivo NIR-PIT on A431 cells, each mouse was randomly divided into six groups of five mice per group when tumors reached 300 to 600 mm^3 and treated with administration of Pan-IR700 (100 μg) i.v. and NIR light illumination at 5, 10, 20, 40, and 80 J/cm^2 at 16 h after injection (Scheme S1C). Mouse urine was carefully collected through 6 h after NIR-PIT in a 1.5 mL sample tube with a pipet. After urine volume was accurately weighed with a pipet, then each sample was diluted 6 times with 1% (v/v) formic acid in methanol (containing 20 μg/L (20 ppb) of IS). After centrifugation at 14,000 rpm at 4 °C for 10 min, the supernatants were transferred into new tubes. The solution was dried by nitrogen spraying and then redissolved in 200 μL of methanol containing 1% formic acid. After centrifugation and transfer of all the supernatant to a polypropylene vial, it was subjected to LC-MS/MS analysis. The amount of ligand was calculated according to the following formula: ligand amount (nmol) = ligand concentration in mouse urine (nmol/mL) × urine volume (mL).

IR700 Fluorescence Imaging. For real-time imaging during NIR-PIT, LIGHTVISION (Shimadzu Corp.), a commercially approved NIR fluorescence imaging system originally designed for measuring ICG fluorescence, was used (collection wavelength of approximately 800 nm). Detailed imaging and analysis methods were performed as described.[13]

Biodistribution Analysis. Based on a previous study, biodistribution analysis was performed immediately before and 0.5, 1, 2, 3, 4.5, 6, 9, 12, and 24 h after administration of 100 μg of Pan-IR700.[7]

Statistical Analysis. Data are presented as the mean ± standard error of the mean (SEM). Statistical analysis was performed with GraphPad Prism version 7 software (GraphPad Software, La Jolla, CA, USA) and LabSolutions software (Shimadzu Corporation). For the analysis of the ligand collection from tumor urine after NIR light illumination, one-way analysis of variance (ANOVA) followed by Dunnett's test was used. Pearson's product moment correlation coefficient was obtained for the correlation between the fluorescence decay ratio and ligand from NIR-PIT-treated-mice's urine. $p < 0.05$ was considered to indicate a statistically significant difference.

■ ASSOCIATED CONTENT

Supporting Information

The Supporting Information is available free of charge at https://pubs.acs.org/doi/10.1021/acsomega.4c09850.

Experimental diagram, LS-MS/MS spectra of real sample of mouse urine, multiple reaction monitoring transitions and LC-MS/MS setting, results of verification of LC-MS/MS ligand analysis method (PDF)

■ AUTHOR INFORMATION

Corresponding Author

Hisataka Kobayashi − *Molecular Imaging Branch, Center for Cancer Research, National Cancer Institute, National Institutes of Health, Bethesda, Maryland 20892, United*

https://doi.org/10.1021/acsomega.4c09850
ACS Omega 2025, 10, 6983−6991

States; orcid.org/0000-0003-1019-4112; Phone: 240-858-3069; Email: kobayash@mail.nih.gov; Fax: 240-541-4527

Authors

Shuhei Okuyama − *Molecular Imaging Branch, Center for Cancer Research, National Cancer Institute, National Institutes of Health, Bethesda, Maryland 20892, United States*

Daiki Fujimura − *Molecular Imaging Branch, Center for Cancer Research, National Cancer Institute, National Institutes of Health, Bethesda, Maryland 20892, United States*

Aki Furusawa − *Molecular Imaging Branch, Center for Cancer Research, National Cancer Institute, National Institutes of Health, Bethesda, Maryland 20892, United States*

Hiroshi Fukushima − *Molecular Imaging Branch, Center for Cancer Research, National Cancer Institute, National Institutes of Health, Bethesda, Maryland 20892, United States*

Ryuhei Okada − *Molecular Imaging Branch, Center for Cancer Research, National Cancer Institute, National Institutes of Health, Bethesda, Maryland 20892, United States*

Tairo Ogura − *Shimadzu Scientific Instruments, Columbia, Maryland 21046, United States*

Masayuki Nishimura − *Shimadzu Scientific Instruments, Columbia, Maryland 21046, United States*

Peter L. Choyke − *Molecular Imaging Branch, Center for Cancer Research, National Cancer Institute, National Institutes of Health, Bethesda, Maryland 20892, United States;* orcid.org/0000-0003-1086-8826

Complete contact information is available at: https://pubs.acs.org/10.1021/acsomega.4c09850

Author Contributions

S.O. and D.F. mainly designed and conducted experiments, performed analysis, and wrote the manuscript; A.F., H.F., R.O., T.O., and M.N. performed experiments and analysis; P.L.C. edited the manuscript and supervised the project; and H.K. planned ana initiated the project, designed and conducted experiments, wrote the manuscript, and supervised the entire project.

Notes

The authors declare no competing financial interest.

■ ACKNOWLEDGMENTS

All authors were supported by the Intramural Research Program of the National Institutes of Health, National Cancer Institute, Center for Cancer Research (ZIABC011513, Funder Id: 10.13039/100000054).

■ ABBREVIATIONS

NIR-PIT, near-infrared photoimmunotherapy; APC, antibody-photoabsorber conjugate; NIR, near-infrared; LC-MS/MS, liquid chromatograph-triple quadrupole mass spectrometer; ICD, immunogenic cell death; EGFR, epidermal growth factor receptor; RECIST, response evaluation criteria in solid tumors; CT, computed tomography; MRI, magnetic resonance imaging; PET, positron emission tomography; ^{18}F-FDG, fluorine-18-fluorodeoxyglucose; HSP, heat shock protein; IS, internal standard; MRM, multiple reaction monitoring; LLOQ, lower limit of quantitation; LQC, low quality control; MQC, middle quality control; HQC, high quality control; SEM, standard error of mean; Pan-IR700, panitumumab-IR700; TBR, tumor-to-background ratio; ANOVA, analysis of variance; ID, injected dose; SUPR, Super Permeability and Retention

■ REFERENCES

(1) Mitsunaga, M.; Ogawa, M.; Kosaka, N.; Rosenblum, L. T.; Choyke, P. L.; Kobayashi, H. Cancer cell-selective in vivo near infrared photoimmunotherapy targeting specific membrane molecules. *Nat. Med.* **2011**, *17* (12), 1685−91.

(2) Kobayashi, H.; Choyke, P. L. Near-Infrared Photoimmunotherapy of Cancer. *Acc. Chem. Res.* **2019**, *52* (8), 2332−2339.

(3) Sato, K.; Ando, K.; Okuyama, S.; Moriguchi, S.; Ogura, T.; Totoki, S.; Hanaoka, H.; Nagaya, T.; Kokawa, R.; Takakura, H.; Nishimura, M.; Hasegawa, Y.; Choyke, P. L.; Ogawa, M.; Kobayashi, H. Photoinduced ligand release from a silicon phthalocyanine dye conjugated with monoclonal antibodies: a mechanism of cancer cell cytotoxicity after near-infrared photoimmunotherapy. *ACS Cent Sci.* **2018**, *4* (11), 1559−1569.

(4) Rakuten Medical, https://rakuten-med.com/us/ (10/24/2024).

(5) https://clinicaltrials.gov/study/NCT03769506 (10/24/2024).

(6) Ogata, F.; Nagaya, T.; Nakamura, Y.; Sato, K.; Okuyama, S.; Maruoka, Y.; Choyke, P. L.; Kobayashi, H. Near-infrared photoimmunotherapy: a comparison of light dosing schedules. *Oncotarget.* **2017**, *8* (21), 35069−35075.

(7) Okada, R.; Kato, T.; Furusawa, A.; Inagaki, F.; Wakiyama, H.; Fujimura, D.; Okuyama, S.; Furumoto, H.; Fukushima, H.; Choyke, P. L.; Kobayashi, H. Selection of antibody and light exposure regimens alters therapeutic effects of EGFR-targeted near-infrared photoimmunotherapy. *Cancer Immunol Immunother.* **2022**, *71* (8), 1877−1887.

(8) Shanbhogue, A. K. P.; Karnad, A. B.; Prasad, S. R. Tumor response evaluation in oncology: current update. *J. Comput. Assist Tomogr.* **2010**, *34* (4), 479−84.

(9) Cai, W. L.; Hong, G. B. Quantitative image analysis for evaluation of tumor response in clinical oncology. *Chronic Dis Transl Med.* **2018**, *4* (1), 18−28.

(10) Cognetti, D. M.; Johnson, J. M.; Curry, J. M.; Kochuparambil, S. T.; McDonald, D.; Mott, F.; Fidler, M. J.; Stenson, K.; Vasan, N. R.; Razaq, M. A.; Campana, J.; Ha, P.; Mann, G.; Ishida, K.; Garcia-Guzman, M.; Biel, M.; Gillenwater, A. M. Phase 1/2a, open-label, multicenter study of RM-1929 photoimmunotherapy in patients with locoregional, recurrent head and neck squamous cell carcinoma. *Head Neck.* **2021**, *43* (12), 3875−3887.

(11) Tahara, M.; Okano, S.; Enokida, T.; Ueda, Y.; Fujisawa, T.; Shinozaki, T.; Tomioka, T.; Okano, W.; Biel, M. A.; Ishida, K.; Hayashi, R. A phase I, single-center, open-label study of RM-1929 photoimmunotherapy in Japanese patients with recurrent head and neck squamous cell carcinoma. *Int. J. Clin Oncol.* **2021**, *26* (10), 1812−1821.

(12) Sano, K.; Mitsunaga, M.; Nakajima, T.; Choyke, P. L.; Kobayashi, H. Acute cytotoxic effects of photoimmunotherapy assessed by ^{18}F-FDG PET. *J. Nucl. Med.* **2013**, *54* (5), 770−5.

(13) Okuyama, S.; Fujimura, D.; Inagaki, F.; Okada, R.; Maruoka, Y.; Wakiyama, H.; Kato, T.; Furusawa, A.; Choyke, P. L.; Kobayashi, H. Real-time IR700 Fluorescence Imaging During Near-infrared Photoimmunotherapy Using a Clinically-approved Camera for Indocyanine Green. *Cancer Diagn Progn.* **2021**, *1* (2), 29−34.

(14) Takashima, K.; Koga, Y.; Anzai, T.; Migita, K.; Yamaguchi, T.; Ishikawa, A.; Sakashita, S.; Yasunaga, M.; Yano, T. Evaluation of Fluorescence Intensity and Antitumor Effect Using Real-Time Imaging in Photoimmunotherapy. *Pharmaceuticals (Basel).* **2022**, *15* (2), 223.

(15) Inagaki, F. F.; Fujimura, D.; Furusawa, A.; Okada, R.; Wakiyama, H.; Kato, T.; Choyke, P. L.; Kobayashi, H. Diagnostic imaging in near-infrared photoimmunotherapy using a commercially available camera for indocyanine green. *Cancer Sci.* **2021**, *112* (3), 1326−1330.

(16) Ogawa, M.; Tomita, Y.; Nakamura, Y.; Lee, M. J.; Lee, S.; Tomita, S.; Nagaya, T.; Sato, K.; Yamauchi, T.; Iwai, H.; Kumar, A.; Haystead, T.; Shroff, H.; Choyke, P. L.; Trepel, J. B.; Kobayashi, H. Immunogenic cancer cell death selectively induced by near infrared photoimmunotherapy initiates host tumor immunity. *Oncotarget.* **2017**, *8* (6), 10425−10436.

(17) Li, H.; Ye, M.; Hu, Z.; Lu, H.; Zheng, D.; Wu, M.; Ge, T.; Xu, S.; Ge, Z.; Zhang, S.; Xu, G.; Chen, H. IKZF3 is a novel prognostic biomarker for head and neck squamous cell carcinoma: A study based on bioinformatics analysis. *Medicine (Baltimore)*. **2023**, *102* (11), No. e33124.
(18) Chen, S.; Yang, Y.; He, S.; Lian, M.; Wang, R.; Fang, J. Review of biomarkers for response to immunotherapy in HNSCC microenvironment. *Front. Oncol.* **2023**, *13*, No. 1037884.
(19) *Bioanalytical Method Validation Guidance for Industry* https://www.fda.gov/media/70858/download 2018.
(20) Chang, A. J.; De Silva, R. A.; Lapi, S. E. Development and characterization of ^{89}Zr-labeled panitumumab for immuno-positron emission tomographic imaging of the epidermal growth factor receptor. *Mol. Imaging.* **2013**, *12* (1), 17−27.
(21) Sato, K.; Watanabe, R.; Hanaoka, H.; Harada, T.; Nakajima, T.; Kim, I.; Paik, C. H.; Choyke, P. L.; Kobayashi, H. Photoimmunotherapy: comparative effectiveness of two monoclonal antibodies targeting the epidermal growth factor receptor. *Mol. Oncol.* **2014**, *8* (3), 620−32.
(22) Weber, W. A. Assessing Tumor Response to Therapy. *J. Nucl. Med.* **2009**, *50* (Suppl 1), 1S−10S.
(23) Mitsunaga, M.; Nakajima, T.; Sano, K.; Choyke, P. L.; Kobayashi, H. Near-infrared theranostic photoimmunotherapy (PIT): repeated exposure of light enhances the effect of immunoconjugate. *Bioconjug Chem.* **2012**, *23* (3), 604−9.
(24) https://classic.clinicaltrials.gov (10/24/2024).
(25) Fujimura, D.; Inagaki, F.; Okada, R.; Rosenberg, A.; Furusawa, A.; Choyke, P. L.; Kobayashi, H. Conjugation Ratio, Light Dose, and pH Affect the Stability of Panitumumab−IR700 for Near-Infrared Photoimmunotherapy. *ACS Med. Chem. Lett.* **2020**, *11* (8), 1598−1604.

https://doi.org/10.1021/acsomega.4c09850
ACS Omega 2025, 10, 6983−6991